

Supplementary abbreviated supine breast MRI following a standard prone breast MRI with single contrast administration: is it effective in detecting the initial contrast-enhancing lesions?

Erkin Aribal 
Onur Buğdaycı 

PURPOSE

We aimed to evaluate the detectability of contrast enhancing lesions, initially demonstrated in standard prone dynamic contrast-enhanced MRI (DCE-MRI), in a supplementary supine breast MRI examination performed following the standard prone DCE-MRI examination and to show the correlation of spatial displacement of the lesions with breast size and density.

METHODS

Forty-two patients with 45 lesions were prospectively evaluated. Supine breast MRI was acquired with a 6-channel body coil following a standard DCE-MRI in prone position after repositioning the patient. No additional contrast media was administered. Images were evaluated by two radiologists in consensus for the visibility of the lesions. Lesion localization relative to the sternal midline, chest wall and nipple was measured in both prone and supine positions. Correlations between lesion displacement and breast size or breast density were analyzed.

RESULTS

Of 45 lesions, 23 (52.3%) were masses, 22 (47.7%) were nonmass enhancements (NME). Forty-four lesions (97.8%) could be detected on supine images. One linear NME of 33 mm in length could not be seen on supine images. Twenty (46.5%) of the detected lesions in supine position were equal to or smaller than 10 mm (11 NME [55%] and 9 masses [45%]). Lesion displacement relative to the chest wall increased with increasing breast size ($P < 0.001$).

CONCLUSION

An abbreviated supine sequence following a standard prone DCE-MRI with single contrast media administration is an effective method for defining the lesion location in supine position.

Magnetic resonance imaging (MRI) of the breast is widely used and has a wide range of indications including the screening of high-risk patients. Dynamic contrast-enhanced MRI (DCE-MRI) has a higher sensitivity and specificity than conventional breast imaging in breast tumor detection (1–5). Prone positioning of the patient is the current practice for breast MRI. Dedicated breast coils are designed for prone imaging which enables the best image quality and definition (6). On the other hand, most of the procedures like ultrasonography (US), biopsy under US guidance, physical examination or breast surgery are performed while the patient is in supine position. This change in body position between procedures can cause large positional displacements of the lesions due to breast deformation and is one of the main challenges in determining the localization of the MRI-only detected lesions (7, 8). A novel technique, volume navigation US with real time co-registration of MRI data, is described in the literature for better localization of these lesions in supine position (9–11). This technique requires an additional supine MRI of the breast with a modified coil and scanning protocol (11). A supplementary supine MRI imaging protocol necessitates repetition of the contrast administration as these lesions are visible only after contrast enhancement. However, a short sequence of supine breast MRI could be added as a supplement following a standard DCE-MRI sequence. This would obviate any additional contrast administration. In this study, we aimed to evaluate the detectability of enhancing lesions, seen initially in prone MRI images, in a supplementary supine breast MRI examination per-

From the Department of Radiology (E.A., O.B. onurbug@hotmail.com), Marmara University School of Medicine, İstanbul, Turkey; Department of Radiology (E.A.), Acibadem Mehmet Ali Aydınlar University School of Medicine, İstanbul, Turkey.

Received 8 April 2018; revision requested 11 June 2018; last revision received 18 November 2018; accepted 10 December 2018.

Published online 24 May 2019.

DOI 10.5152/dir.2019.18167

You may cite this article as: Aribal E, Buğdaycı O. Supplementary abbreviated supine breast MRI following a standard prone breast MRI with single contrast administration: is it effective in detecting the initial contrast-enhancing lesions? *Diagn Interv Radiol* 2019; 25:265–269.

formed following a standard prone DCE-MRI examination and to show the correlation of spatial displacement of the lesions with breast size and density.

Methods

Patients

This study was approved by our institutional ethics committee (Approval number 09.2017.143). Patients were recruited from December 1, 2016 to January 1, 2017. All patients who had a DCE-MRI examination of the breast during this period were included in the study. Eighty-seven patients with different breast MRI indications were examined. The indications included screening, preoperative staging, and evaluation of difficult cases that were not solved by conventional imaging methods. Exclusion criteria were: (i) patients refusing to enter the study; (ii) patients who could not complete the routine prone breast MRI examination due to several reasons like claustrophobia or contrast media reaction. One patient was excluded due to motion artifacts on both prone and supine MRI. Eighty-six patients were evaluated. The mean age was 47.61 ± 10.82 years, ranging from 21 to 77 years. Forty-two of 86 patients had 45 contrast enhancing lesions. The remaining 44 patients did not show any enhancing lesion on the standard prone DCE-MRI; consequently, the supine examination of these patients was not evaluated. The mean age for the patients with lesions was 47.22 ± 11.08 years (range, 21–77 years) and those without lesions was 47.94 ± 10.54 years (range, 25–70 years).

Standard prone breast MRI examination

Standard clinical breast MRI protocol was acquired using a 3 Tesla scanner (Magnetom

Verio, Siemens Healthcare) with the patient in prone position with a 16-channel phased-array dedicated breast coil (Siemens Healthcare). Examination protocol comprised following sequences: 1) Axial turbo spin-echo fat saturated T2-weighted sequence (TR/TE, 4100/70 ms; field of view, 30 cm; acquisition matrix, 440×380 ; slice thickness, 3 mm; and acquisition time, 3 min 43 s). 2) Diffusion-weighted imaging using echo-planar image (EPI) sequence with fat suppression (*b* values 50, 400 and 800 s/mm^2 ; TR/TE, 9700/86 ms; FOV, 30 cm; in-plane resolution, 1.7×2 mm²; slice thickness, 3 mm; and acquisition time, 4 min 32 s). 3) 3D volumetric interpolated (VIBE) sequence (TR/TE, 5.01/1.77 ms; FOV, 30 cm; acquisition matrix, 512×460 ; slice thickness, 1 mm; in-plane resolution, $0.6 \times 0.7 \times 1.0$ mm; and total acquisition time, 10 min with a temporal resolution of 82 s) for dynamic contrast-enhanced sequence. Contrast agent, Gadobutrol 0.1 mmol/kg (Bayer Schering Pharma AG), or Gadoterate Meglubine 0.1 mmol/kg (Guerbet) were administered intravenously via an antecubital vein at a rate of 2 mL/s using an automated injector system (Medrad Spectris Solaris EP, Bayer Medical Care) followed by a saline injection. Subtracted contrast-enhanced dynamic images were used as standard for lesion identification.

Supine breast imaging

After completion of the prone breast MRI the patient was taken out of the magnet. The dedicated breast coil was retrieved. Patient position was changed to supine with both arms extended over the head. A flexible 6-channel body coil (Body Matrix Coil, Siemens Healthcare) was centralized on the sternum and placed over both breasts and was fixed with a strap to prevent coil displacement and minimize artifacts due to respiratory motion. A single three-dimensional turbo field echo sequence was used for T1-weighted high resolution examination volume without fat suppression (TR/TE, 2030/12 ms; flip angle, 120 degrees; field of view, 320 mm; matrix, 322×480 mm; acquisition time, 82 s). The whole procedure time was 2 min 20 s. The mean time spent in between prone and supine MRI for the patient repositioning was 70 s (range, 60–85 s). The duration of the whole procedure with the patient repositioning and acquisition of pilot images was 3 min 10 s. The T1-weighted acquisition was started (on average) 12 min 20 s after the initial contrast administration.

Evaluation of the images

Prone and supine MRI were then compared using commercial PACS software (Infiniti Healthcare). Lesions were first located in standard prone MRI, and then sought for in supine MRI (Fig. 1). Subtracted images in the standard prone images were evaluated first, followed by original non fat-saturated T1-weighted contrast-enhanced sequences. Two reviewers evaluated the images in consensus. Lesion size was measured as the longest diameter in any orthogonal plane. Lesion location was recorded in quadrants. The distances of the lesion from the sternum, the chest wall and the nipple were measured separately. The measurements were done as follows: for the measurements from the lesion to sternum, a horizontal line from the center of the lesion to the sternal midline was drawn; for the distance to the chest wall, a perpendicular line to the chest wall was drawn from the center of the lesion; for the distance to the nipple, a line was drawn from the center of the lesion to the nipple on a sagittal oblique reformat image including both the lesion and the nipple. We measured the breast sizes on axial prone image passing through the nipple. A free-hand line was drawn around the breast to measure the breast area on the slice. The breast fibroglandular tissue composition was assessed according to ACR recommendations (12).

Statistical analysis

Data analysis was performed using SPSS Statistics v22 (IBM Corp.) statistical software. Kolmogorov-Smirnov test was used to analyze normality of data and nonparametric tests were used, in addition to descriptive statistics. Spearman's correlation test was used to look for correlations between breast area and lesion displacement and between lesion location and lesion displacement. Independent sample t-test was performed to look for association between breast density and lesion displacement. $P < 0.05$ was used as the cutoff to infer statistical significance.

Results

Forty-two of 86 patients had 45 lesions. Twenty-three (52.3%) of these lesions were masses and 22 (47.7%) had nonmass enhancement (NME). The mean lesion size was 14.47 ± 11.11 mm (range, 3–59 mm). The mean size for masses was 14.29 ± 7.88 mm (range, 6–34 mm) and 14.68 ± 14.20 mm (range, 3–59 mm) for NMEs. Twenty (46.5%) of the detected lesions in supine

Main points

- Prone breast MRI detected lesions can be challenging to relocate on supine body position due to significant displacement of these lesions and deformation of the breast tissue in supine position. This problem can be substantially overcome with a supplementary supine imaging obtained following a standard MRI.
- Almost all lesions can still be detected several minutes after contrast material injection on a supplemental supine MRI.
- Lesion displacement according to the chest wall was correlated with breast size.

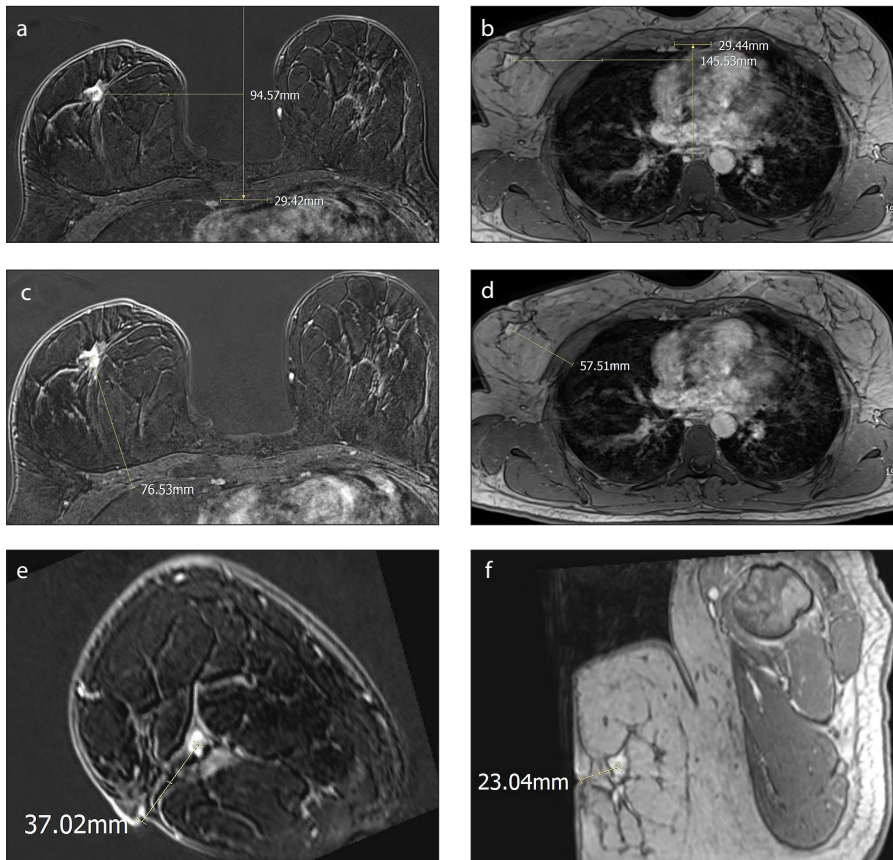


Figure 1. a–f. A 54-year-old woman with invasive ductal carcinoma. Lesion displacement measurements in prone (a, c, e) and supine (b, d, f) images. The distance of the lesion to the sternum (a, b), chest wall (c, d), and the nipple (e, f) were measured. Sagittal oblique reformatted images (e, f) show the lesion and nipple in the same plane.

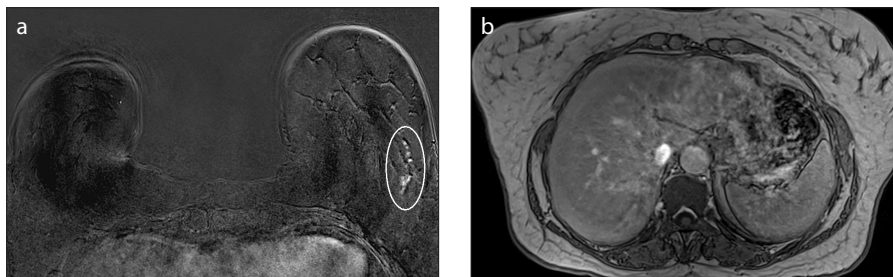


Figure 2. a, b. A 56-year-old woman with ductal carcinoma in situ. The only lesion not seen in supine images was a linear NME of 33 mm in length. Linear NME in the left breast (circled) seen in prone image (a). The lesion could not be seen in supine images (b).

Table 1. Changes in distance from sternum, chest wall, and nipple when moving from prone to supine position (calculated as distance in prone position - distance in supine position)

	Range	Minimum	Maximum	Mean
Change in distance to sternum	-81	3	-78	-34.8
Change in distance to chest wall	132	-36	96	29
Change in distance to nipple	109	-47	62	-14.7

position were ≤ 10 mm (11 NME [55%] and 9 masses [45%]). Twenty-eight of 45 lesions showed benign histopathology (14 benign changes, 14 fibroadenoma) and remaining

17 were malignant (8 ductal carcinoma in situ and 9 invasive ductal cancer). The mean breast area was 10798 ± 5590.79 mm², ranging from 1708 to 22351 mm².

We were not able to define one lesion in one patient in the supine images. The lesion was NME and the size of the lesion was 33 mm (Fig. 2). The remaining 44 lesions (97.8%) were detected in supine images.

Fibroglandular breast patterns of the breasts with those 44 lesions were type A in two (4.5%), type B in 16 (36.4%), type C in 16 (36.4%) and type D in 10 (22.7%) patients. Due to the small number of patients with type A fibroglandular breast composition, fibroglandular tissue composition was grouped as nondense (types A and B) and dense (types C and D).

Twenty-two lesions (50%) were located in the upper outer quadrant, 8 lesions (18.2%) were located in the upper inner quadrant, and 14 lesions (31.8%) were located in the lower outer quadrant.

Table 1 shows changes in distance from sternum, chest wall, and nipple when moving from prone to supine position. Lesions moved mostly away from the sternum and towards the chest wall due to the position change.

Lesion displacement relative to the chest wall and breast size were moderately correlated ($r_s = 0.527$, $P < 0.001$) (Table 2). Displacement increased in larger breasts (Fig. 3). There was no correlation between lesion displacement relative to the chest wall and fibroglandular tissue composition ($P = 0.34$) (Table 3). There was no correlation between lesion displacement relative to the nipple and breast size ($r_s = 0.185$, $P = 0.23$) or fibroglandular tissue composition ($P = 0.16$). There was also no correlation between lesion displacement from sternal midline and breast size ($r_s = 0.092$, $P = 0.55$) or breast fibroglandular tissue composition ($P = 0.91$). There was no correlation between lesion location within the breast and the amount of lesion displacement relative to the chest wall, nipple, or sternal midline (Table 1).

Discussion

The present study showed that 97.8% of the lesions can be depicted on a supplementary abbreviated supine MRI examination following a standard diagnostic prone DCE-MRI with a single contrast administration. One lesion (2.2%) that was not detected on supine MRI was a 33 mm ductal carcinoma in situ presenting as NME. However, we were able to detect all lesions smaller than 10 mm (46.7%), which pose a bigger challenge in second-look US (13). The mean time spent for this supplementary method

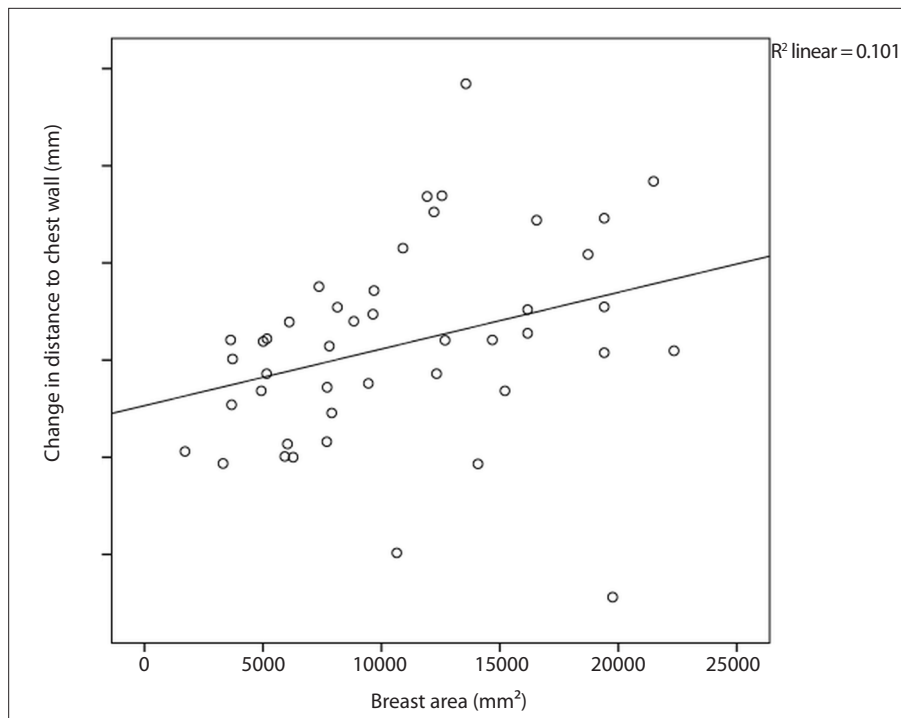


Figure 3. Scatterplot showing the association between breast area and lesion displacement relative to the chest wall.

Table 2. Correlation of change in distance to sternum, nipple, and chest wall between breast size and lesion location

	Breast size		Lesion location	
	Rho	P	Rho	P
Change in distance to sternum	0.092	0.55	-0.098	0.53
Change in distance to nipple	0.185	0.23	-0.139	0.37
Change in distance to chest wall	0.527	<0.001	0.072	0.64

Table 3. Change in distance to sternum, nipple, and chest wall according to breast patterns

Breast pattern	Change in distance to sternum	Change in distance to nipple	Change in distance to chest wall
	Mean±SD	Mean±SD	Mean±SD
Nondense (n=18)	35.2±21.6	19.7±16.2	33.5±25.8
Dense (n=26)	34.6±15.1	11.3±21.1	25.9±25.6
P*	0.91	0.16	0.34

SD, standard deviation.
*Independent sample t test.

was 3 min 10 s including the patient repositioning and coil placement. This supplementary sequence was performed approximately 11 minutes after the initial contrast injection.

To our knowledge there is not a similar study in the literature. However, a previ-

ous study with prone imaging showed 97% overall sensitivity with a delayed contrast-enhanced sequence 6–9 min after contrast injection (14). On the other hand, value of supine imaging after a standard prone protocol was not evaluated. In a previous study (15), 6 breast cancer patients

were studied with supine breast MRI both in pre- and postoperative period with a 3 T intraoperative MRI. They reported deformation of the lesions due to change from prone to supine position. They observed an average change of 23.8% in the measured volume of the tumor and 16.2% change in compactness (15).

This study showed that a delayed sequence was effective in depicting the prone MRI detected lesions (97.8% of the cases). Thus, a delayed supine imaging after the standard MRI protocol will enable ready supine images. Showing the deformation and displacement of the lesion will be useful for further clinical work, i.e., second-look US examination, surgery planning. The success rate of second-look US is variable (16). A recent meta-analysis showed a markedly heterogeneous detection rate with second-look US ranging between 23% and 81.2% (15). This analysis showed that mass and malignant lesions were more likely to be detected on second-look US (66% and 79%, respectively) compared to NMEs (29%). However, they stated a 12.2% likelihood of malignancy in cases where second-look US did not detect any lesions (15). On the other hand, the lesion that is detected on second-look US may not be the real matching lesion seen on prone MRI due to the deformation and relocation of the lesions in supine position. A supine examination can be used as a guiding tool for these incidents. A new technique, i.e., volume navigation US imaging with real-time co-registration of the MRI data is used in different clinical settings for second-look US or guidance for breast biopsy (17, 18). This technique requires contrast-enhanced supine MRI of the breast which necessitates an additional MRI examination and contrast administration (11). On the other hand, in some centers supine MRI is used as a guiding method for the preoperative evaluation of breast cancer (15).

Our results were in line with the literature in terms of lesion dislocation despite the different measurement method used in our study (15). Lesions mostly moved laterally and towards the chest wall when the position is changed from prone to supine. Additionally, we found a decrease in nipple to lesion distance in supine position. The displacement towards the chest wall was correlated with breast size.

This study has some limitations. First, we did not assess the interobserver variability in defining the lesions on supine MRI sequences. Second, our study population was

small. Third, both readers observed the deformation of the lesions in supine images; however, we did not assess the deformation of the lesions or breast tissue methodically. Change of position from prone to supine causes both lesion distortion and displacement (15). Tumor location change from prone to supine position has been studied with prone MRI and supine computed tomography examinations (8). It was reported that factors affecting the breast movements other than the inner-lower quadrant were complicated and could not be predicted. But for the inner lower quadrant, the researchers defined the tumor motion radially toward the center of the nipple with the patient position change from prone to supine (8). Most breast lesions are in the outer quadrants of the breast and unpredictable movement of these lesions from prone to supine body position poses a challenge for defining them on second-look US examination. Using anatomical landmarks like the nipple is one of the methods to overcome these positional differences (7, 13). We believe that further studies with a larger patient population evaluating the detectability of lesions with various characteristics and the deformation of both masses and NMEs will be informative.

In conclusion, an abbreviated supine sequence following a standard diagnostic prone MRI examination with single contrast media administration is an effective method in defining the lesion location on supine body position and can be used for further procedures like second-look US, volume navigation US, or surgery. We believe that this abbreviated supplemental examination will not cause too much incremental time cost for the MRI schedules, if the patients who will get benefit from this supplemental sequence are chosen correctly. Lesion displacement according to the chest wall was correlated with breast size. However, there was no correlation between breast size and

lesion displacement relative to the distance to sternum or nipple. The amount of fibroglandular tissue had no significant effect on lesion displacement within the breast.

Acknowledgments

The authors would like to thank Dr. Cemal Aydın Gündoğmuş for his help in creating this article.

Conflict of interest disclosure

The authors declared no conflicts of interest.

References

1. Morris EA. Diagnostic breast MR imaging: current status and future directions. *Radiol Clin North Am* 2007; 45:863–880. [\[CrossRef\]](#)
2. Warner E, Messersmith H, Causer P, et al. Systematic review: using magnetic resonance imaging to screen women at high risk for breast cancer. *Ann Intern Med* 2008; 148:671–679. [\[CrossRef\]](#)
3. Aribal E, Asadov R, Ramazan A, et al. Multiparametric breast MRI with 3T: Effectivity of combination of contrast enhanced MRI, DWI and 1H single voxel spectroscopy in differentiation of Breast tumors. *Eur J Radiol* 2016; 85:979–986. [\[CrossRef\]](#)
4. Rahbar H, Partridge SC. Multiparametric MR imaging of breast cancer. *Magn Reson Imaging Clin N Am* 2016; 24:223–238. [\[CrossRef\]](#)
5. Kuhl CK, Strobil K, Bieling H, et al. Supplemental Breast MR Imaging Screening of Women with Average Risk of Breast Cancer. *Radiology* 2017; 283:361–370. [\[CrossRef\]](#)
6. Mann RM, Kuhl CK, Kinkel K, et al. Breast MRI: guidelines from the European society of breast imaging. *Eur Radiol* 2008; 18:1307–1318. [\[CrossRef\]](#)
7. Carbonaro LA, Tannaphai P, Trimboli RM, et al. Contrast enhanced breast MRI: spatial displacement from prone to supine patient's position. Preliminary results. *Eur J Radiol* 2012; 81:e771–e774. [\[CrossRef\]](#)
8. Satake H, Ishigaki S, Kitano M, et al. Prediction of prone-to-supine tumor displacement in the breast using patient position change: investigation with prone MRI and supine CT. *Breast Cancer* 2016; 23:149–158. [\[CrossRef\]](#)
9. Fausto A, Rizzato G, Preziosa A, et al. A new method to combine contrast-enhanced magnetic resonance imaging during live ultrasound of the breast using volume navigation technique: a study for evaluating feasibility, accuracy and reproducibility in healthy volunteers. *Eur J Radiol* 2012; 81:e332–e337. [\[CrossRef\]](#)

10. Nakano S, Kousaka J, Fujii K, et al. Impact of real-time virtual sonography, a coordinated sonography and MRI system that uses an image fusion technique, on the sonographic evaluation of MRI-detected lesions of the breast in second-look sonography. *Breast Cancer Res Treat* 2012; 134:1179–1188. [\[CrossRef\]](#)
11. Kucukkaya F, Aribal E, Tureli D, et al. Use of a volume navigation technique for combining real-time ultrasound and contrast-enhanced MRI: accuracy and feasibility of a novel technique for locating breast lesions. *AJR Am J Roentgenol* 2015; 206:217–225. [\[CrossRef\]](#)
12. Morris EA, Comstock CE, Lee CH. ACR BI-RADS® Magnetic Resonance Imaging. ACR BI-RADS® Atlas, Breast Imaging Reporting and Data System. Reston, VA: American College of Radiology; 2013.
13. Park VY, Kim MJ, Kim E-K, et al. Second-look US: how to find breast lesions with a suspicious MR imaging appearance. *Radiographics* 2013; 33:1361–1375. [\[CrossRef\]](#)
14. Leong CS, Daniel BL, Herfkens RJ, et al. Characterization of breast lesion morphology with delayed 3DSSMT: an adjunct to dynamic breast MRI. *JMRI* 2000; 11:87–96.
15. Spick C, Baltzer PA. Diagnostic utility of second-look US for breast lesions identified at MR imaging: systematic review and meta-analysis. *Radiology* 2014; 273:401–409. [\[CrossRef\]](#)
16. Pons EP, Azcón FM, Casas MC, et al. Real-time MRI navigated US: role in diagnosis and guided biopsy of incidental breast lesions and axillary lymph nodes detected on breast MRI but not on second look US. *Eur J Radiol* 2014; 83:942–950. [\[CrossRef\]](#)
17. Aribal E, Tureli D, Kucukkaya F, et al. volume navigation technique for ultrasound-guided biopsy of breast lesions detected only at MRI. *AJR Am J Roentgenol* 2017; 208:1400–1409. [\[CrossRef\]](#)
18. Gombos EC, Jayender J, Richman DM, et al. Intraoperative supine breast MR imaging to quantify tumor deformation and detection of residual breast cancer: preliminary results. *Radiology* 2016; 281:720–729. [\[CrossRef\]](#)